Slowdown of thermalization and the emergence of prethermal dynamics in disordered optical lattices

Georgios G. Pyrialakos,[1,2] Fan O. Wu,[2] Pawel S. Jung,[2] Huizhong Ren,[1] Konstantinos G. Makris,[3] Ziad H. Musslimani,[4] Mercedeh Khajavikhan,[1] Tsampikos Kottos,[5] and Demetrios Christodoulides[1,*]

[1]*Ming Hsieh Department of Electrical and Computer Engineering, University of Southern California, Los Angeles, California 90089, USA*
[2]*CREOL, The College of Optics and Photonics, University of Central Florida, Orlando, Florida 32816, USA*
[3]*ICTP, Department of Physics, University of Crete, 71003 Heraklion, Greece*
[4]*Department of Mathematics, Florida State University, Tallahassee, Florida 32306-4510, USA*
[5]*Department of Physics, Wesleyan University, Middletown, Connecticut 06457, USA*

(Received 16 June 2023; revised 30 November 2023; accepted 10 December 2023; published 19 January 2024)

By utilizing the theoretical tools of optical thermodynamics, we investigate thermalization in nonlinear disordered lattices beyond the diffusion regime. Even under extreme levels of disorder, we analytically predict the expected thermal value of entropy and the associated Rayleigh-Jeans distribution, once thermalization ensues. In this context, we reveal a crossover point of disorder beyond which we observe a pronounced slowdown of thermalization in a regime characterized by a logarithmic scaling of equilibration times. By employing the same analytical and numerical tools, we investigate the scaling of thermalization times with respect to both the number of sites and optical temperatures. By exploring the physics of the underlying nonequilibrium response, we unveil a multitude of emerging thermal phenomena, including the development of prethermal Rayleigh-Jeans states in the presence of an optical heat bath and the deceleration of self-heating in Floquet photonic lattices.

DOI: 10.1103/PhysRevResearch.6.013072

I. INTRODUCTION

Ever since Anderson's groundbreaking prediction that randomness in a lattice can give rise to localized eigenstates and inhibit transport, the exploration of disordered systems has unveiled a diversity of intriguing phenomena [1–5]. In photonics, while disorder can provide new means in manipulating light [6–9], it must frequently coexist with nonlinearity, as typically encountered in laser systems or optical waveguides [10–16]. In such context, the dynamics of disordered systems become exceedingly complex, especially when attempting to predict the evolution of localized wave packets, typically associated with a remarkably slow diffusion process [17–20]. While this process is directly relevant to the interplay between disorder and nonlinearity, it provides only a limited view of the asymptotic response of disordered systems.

To comprehensively understand the response of disordered nonlinear settings, it would be necessary to deploy tools from statistical mechanics and thermodynamics. In this context, predicting the onset of thermalization in disordered nonlinear systems, like those described by nonlinear Schrödinger type models (NLSE) [21–24], poses a formidable challenge as analytical indicators of equilibration are not always clearly defined. Traditionally, thermalization has been predicted by observing a distribution akin to a Gibbs ensemble (by using fitting parameters), or simply by observing wave-packet diffusion [20,25–28]. In most cases, this problem is addressed by employing arbitrary metrics for entropy growth and extraction of temperature. However, to employ the maximization of entropy as a reliable measure requires a precise definition of the entropy's thermal value (i.e., its value at equilibrium). This, in turn, requires knowledge of all equilibrium properties, from arbitrary initial conditions, as well as a rigorous expression for the entropy itself.

In this study, we employ the theoretical framework of optical thermodynamics [29–36] to study the nonlinear dynamics of disordered photonic systems beyond the diffusion regime. By introducing a formal scheme, we predict the average modal distribution at equilibrium and the associated thermal value of the optical entropy. In this regard, we ultimately provide precise criteria for numerically evaluating the speed of thermal relaxation into a maximum (thermal) entropy state. We show that a strong disorder leads to a pronounced slowdown of thermalization times above a localization crossover point, signifying a logarithmic scaling regime with unique nonequilibrium dynamics, dominated by long-lived modal oscillations. We further investigate settings where the optical energy is not dynamically conserved. Under slowly varying conditions, we analytically calculate the optical temperature from the instantaneous value of energy, thereby predicting stable prethermal Raylegh-Jeans states, even under extreme disorder. We illustrate these results in a disordered optical system coupled to a heat bath and a self-heating Floquet lattice.

*demetri@usc.edu

A. Thermalization dynamics in disordered optical lattices

We investigate photonic disordered lattices through the lens of optical thermodynamics by considering a generalized square lattice of size $M_x \times M_y$, governed by

$$i\partial_t a_{ij} = \beta_{ij} a_{ij} + |a_{ij}|^2 a_{ij} + \sum_{k}^{M_x} \sum_{l}^{M_y} \kappa_{ij,kl} a_{kl}, \tag{1}$$

where i, j, k, l are spatial site indices (i, k towards x and j, l towards y), β_{ij} represent on-site potentials, and $\kappa_{ij,kl}$ are coupling or exchange coefficients. The second term on the right side describes Kerr-type nonlinear effects. Here, we consider two types of disordered lattices, in one dimension and two dimensions. The first one corresponds to an Anderson system with on-site randomness $\beta_{ij} = \Lambda A_{ij,\xi}$ where Λ is the disorder strength and $A_{ij,\xi}$ is a bounded random Anderson potential with a possible spatial correlation length ξ. The second arrangement corresponds to an Aubry-André (AA) potential with a randomness in each direction $\Lambda[\cos(2\pi a i + \phi)]$ where the spatial frequency a is a good irrational number that guarantees aperiodicity. We note that for this system the AA localization-delocalization threshold is $\Lambda = 2$ [37].

In Eq. (1), eigenmode localization is tied to the disorder introduced in β_{ij}, while the Kerr operator acts as a mechanism that drives the system into thermalization by promoting a chaotic power exchange between the eigenmodes. Here, the vector a_{ij} can be expanded using the linear eigenmode basis, as $a_{ij}(t) = \sum_n c_n(t) e^{-i\epsilon_n t} u_{n,ij}$ where $u_{n,ij}$ are the eigenmode field profiles, $c_n(t)$ represent the complex modal occupancies, and ϵ_n are the eigenvalues. A fundamental axiom of optical thermodynamics dictates that state evolution must occur ergodically in phase space in the presence of invariant quantities. For an isolated and fully conservative optical arrangement like the ones considered here, two invariants are at play: the optical power $P = \sum_n |c_n|^2$ and the optical energy $U = -\sum_n \epsilon_n |c_n|^2$ which corresponds to the linear part of the total Hamiltonian $H^{\text{tot}} = U + H^{NL}$ (H^{tot} is an exact invariant of motion), where the fluctuations of H^{NL} are assumed negligible in the weakly nonlinear regime. Under these conditions the system eventually relaxes into a Rayleigh-Jeans (RJ) distribution [29,38,39], given by

$$\langle |c_n|^2 \rangle = -T/(\varepsilon_n + \mu), \tag{2}$$

where T and μ represent, respectively, the optical temperature and chemical potential of the system (see Appendix A). In this respect, the theory of optical thermodynamics allows one to calculate the optical temperature and chemical potential in Eq. (2) for any arbitrary initial conditions (with known U, P). This is accomplished by solving a system of two equations, namely, the equation of state, $U - \mu P = MT$, and the equation for power, $P = \sum_n |c_n|^2$, after substituting Eq. (2) [29]. Moreover, one can associate any input conditions to a thermal value of the optical entropy, given by $S = \sum_n \log |c_n|^2$, which is equivalent to

$$S_{TH} = \sum_n \log [-T/(\varepsilon_n + \mu)]. \tag{3}$$

The latter expression provides a precise criterion for equilibration, for any disordered optical system in the weakly nonlinear regime. In other words, it furnishes a definite value based on which one can determine in a definitive manner whether a system has thermally relaxed or not. This aspect is particularly important for disordered lattices, given their extremely slow relaxation dynamics and quasi-random spectral properties.

In general, the strength of couplings, the strength of nonlinearity, and the level of disorder enter on equal footing in Eq. (1). Therefore, in the following, we normalize the former two and consider only Λ as a free parameter. In this regard, we identify three key variables that can influence the speed of thermalization, namely, the disorder strength Λ, the number of sites M, and the expected RJ temperature T. By employing Eq. (3) as our absolute metric for thermal equilibrium, we declare the onset of thermalization when the condition $S_p = [S(t) - S_{TH}]/[S(0) - S_{TH}] \lesssim 0.02$ is met.

To investigate the scaling with respect to Λ, we examine four Anderson and Aubry-André lattices [$a = \sqrt{(19/50)}, \phi = \pi/5$], in one-dimensional (1D) and two-dimensional (2D) configurations, involving 30 and 400 sites, respectively. The results are averaged over $N_a = 200$ ensembles, when keeping U and P constant. In Fig. 2(a) we identify a threshold that signifies a transition to a universal logarithmic scaling regime of thermalization times, characterized by a significant slowdown of mode mixing, after $\Lambda = 2$. As we will demonstrate, this value is linked to a crossover in the nonlinear wave-mixing dynamics, correlated with the degree of eigenmode localization. In general, claiming universality for $\Lambda = 2$ can be challenging. However, considering that the lattices under study generally display comparable levels of eigenmode localization at this level of disorder, it is anticipated that thermalization times will diverge in a similar manner.

In Figs. 2(b) and 2(c) we plot thermalization times for the 1D Anderson lattice with respect to the number of sites and the expected RJ temperature, respectively. A general rule of thumb for optical systems with zero disorder is that thermalization times scale with P/M. Here, we find this to hold true even for high disorder levels where a flat scaling regime emerges. The results of Fig. 2(b) are extracted by initiating the lattices at an identical eigenvalue window (forcing a specific T) with total power $P = P_0 M$ and $S_p \lesssim 0.05$. Next, we monitor thermalization times ($S_p \lesssim 0.02$) as the temperature varies from 0 to $\pm\infty$. We observe that thermalization times increase logarithmically as the temperature drops. At lower temperatures, the RJ distribution involves only a few modes with closely spaced eigenvalues at the tail of the spectrum. This limits the mode-mixing pathways, as these modes tend to be randomly localized at distinct sites of the lattice (that are typically far apart) under high disorder.

In order to gain a deeper understanding of this scaling behavior, we focus on the following equation:

$$i\partial_t c_n = \sum_{n_1,n_2,n_3} V_n^{n_1,n_2,n_3} c_{n_1}^* c_{n_2} c_{n_3} e^{i(\epsilon_n + \epsilon_{n_1} - \epsilon_{n_2} - \epsilon_{n_3})t}, \tag{4}$$

which describes the evolution of the modal occupancies, obtained by projecting Eq. (1) onto the linear modal basis. Here, $V_n^{n_1,n_2,n_3} = \sum_{ij} u_n u_{n_1} u_{n_2} u_{n_3}$ correspond to the four-wave mixing overlap integrals of the involved eigenmodes (with indices n, n_1, n_2, and n_3). In general, the degree of power exchange

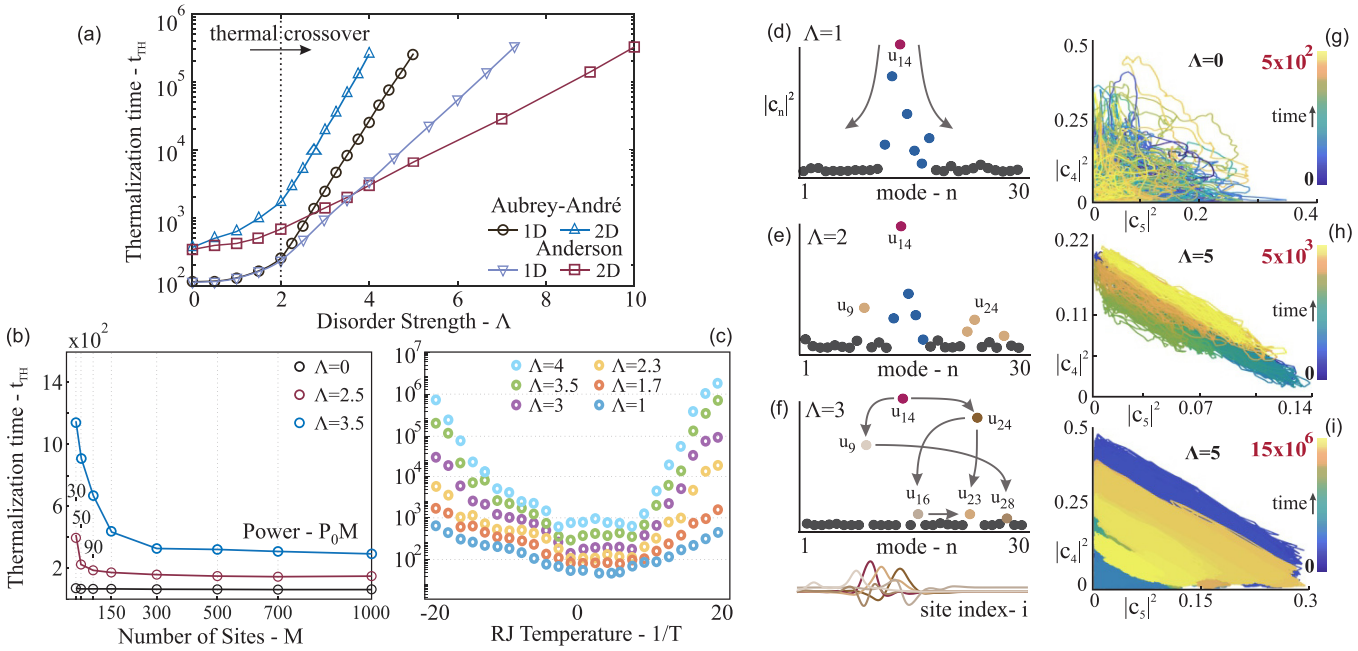

FIG. 1. Relaxation times as a function of (a) disorder strengths for four different lattices initiated out of equilibrium, (b) the number of sites for a 1D Anderson lattice, and (c) temperature for the same lattice. (d)–(f) Average modal occupancies for a 30-site Aubry-André lattice for different disorder strengths, at time $t = 10$. The lattice is initiated by exciting only one eigenmode (u_{14}). At $\Lambda = 2$ a crossover threshold exists that separates the ballistic ($\Lambda = 1$) and the localized regime ($\Lambda = 3$). (g)–(i) Phase space trajectories in the subspace spanned by the modal occupancies $|c_4|^2$ and $|c_5|^2$.

between different modes in the presence of nonlinearity is determined by two key factors: the degree of phase matching and the level of spatial overlapping, dictated by V_n. In a lattice with extended (nonlocalized) eigenmodes, the V_n amplitudes are comparable for all different possible combinations of the n, n_1, n_2, n_3 mode indices. In this respect, it is expected that the strength of the mode-mixing process will be primarily determined by the phase matching condition of the eigenvalues. Here, phase matching is attained if $\epsilon_n + \epsilon_{n_1} - \epsilon_{n_2} - \epsilon_{n_3} \approx 0$. Under this condition, the exponential term will vary slowly, thus allowing this particular combination of modes to exchange power. Otherwise, this nonlinear exchange is considerably suppressed.

In Figs. 1(d)–1(f) we plot the modal amplitudes of the 1D Aubry-André lattice subjected to different levels of disorder. We initially excite only the 14th supermode, u_{14}, with the index n being in ascending order, from the lowest to the highest eigenevalue. For $\Lambda = 1$, and after $t = 10$, we can observe that power has spread "diffusively" into the nearest eigenmodes in the ϵ_n axis [Fig. 2(d)], a process that is expected to persist until a RJ distribution is formed. This signifies the dominant role of phase matching in thermalization for low disorder levels. On the other hand, under strong disorder ($\Lambda = 3$), mode overlapping overtakes phase matching as the dominant mechanism. In this case, the overlap integrals V_n will be effectively nonzero only for combinations of modes that are tightly localized in neighboring sites. Indeed, in Fig. 1(e) we notice that power was primarily exchanged between modes that are physically nearest in the discrete lattice space indexed by i, irrespective of their distance in the ϵ_n axis. Of interest would be to observe what happens exactly at the crossover threshold of the Aubry-André lattice. Here, for $\Lambda = 2$, we notice that power has been equally exchanged between modes that are both nearest in the ϵ_n axis as well as between neighboring quasi-localized states. This point coincides with the crossover in the logarithmic scaling regime.

It is apparent that, in this logarithmic domain, each mode exhibits effectively a nonzero V_n only when paired with other neighboring modes. A strong indicator of the transition between these two regimes is an oscillatory dynamical response in modal space, a behavior reminiscent of chaotic spots [25]. To illustrate this behavior, we plot the nonlinear evolution for the 30-site Aubry-André lattice in a reduced phase space spanned by the modal occupancies of u_4 and u_5 [Figs. 2(g)–2(h)]. The lattice is initiated by populating only these two modes, selected on purpose because they exhibit strong nonlinear coupling due to their localization in neighboring sites. For $\Lambda = 0$ we observe fully chaotic dynamics where after a short observation time ($t = 510^2$), the system succeeds in exploring its full phase space rapidly, in an ergodic fashion. On the other hand, for a strong disorder at $\Lambda = 5$, we observe perpetual oscillations between u_4 and u_5 with a slowly varying amplitude. For this level of disorder, to achieve full coverage of the phase space, evolution times must exceed the time mark of $t = 1510^6$ [as shown in Fig. 2(i)], when thermalization ultimately ensues.

II. NONEQUILIBRIUM DYNAMICS AND EMERGENCE OF MODAL OSCILLATIONS

By monitoring the thermal relaxation of strongly disordered lattices we can show that classical localization can indeed deeply suppress thermalization times. However, we need to provide a decisive argument for the success of

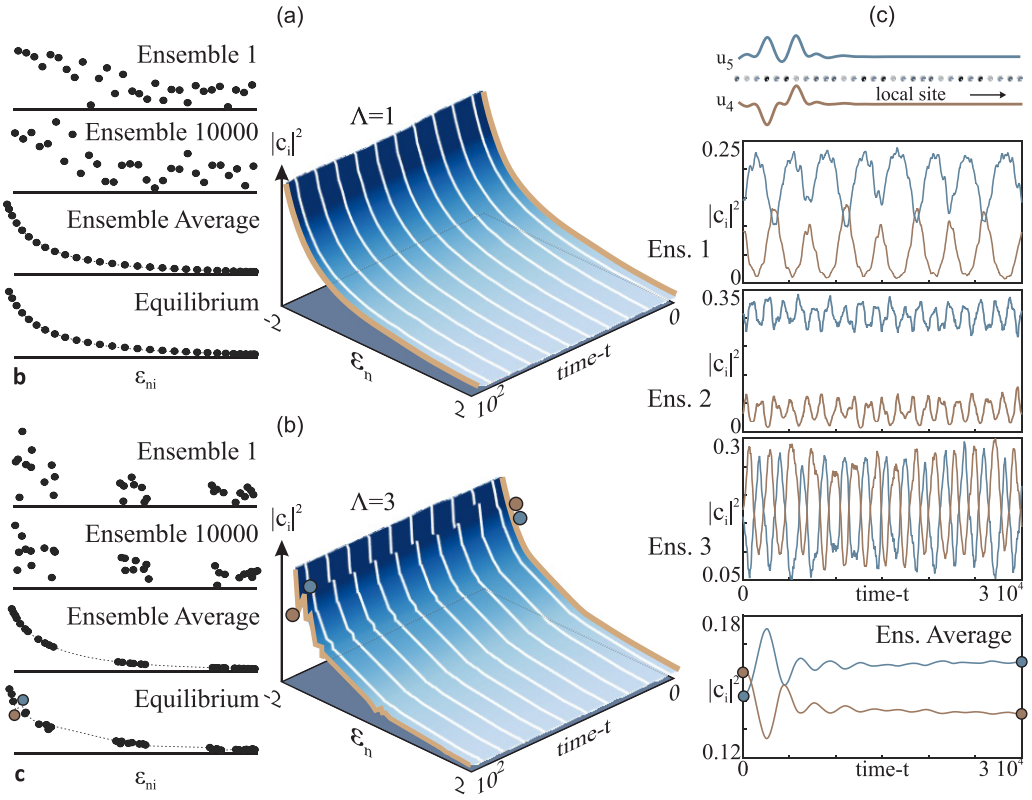

FIG. 2. (a) A weakly disordered Aubry-André lattice ($\Lambda = 1$) is excited very close to its thermal equilibrium by randomly initiating each ensemble at $U = 2.3$ and $P = 2$. The ensemble average at $t = 0$ and at $t = 10^2$ corresponds to the same RJ distribution without demonstrating any deviations from this thermal equilibrium. (b) A strongly disordered Aubry-André lattice ($\Lambda = 5$) can escape thermal equilibrium. This effect is driven by the strong mutual coupling between particular pairs of eigenmodes. (c) Two eigenmodes that are localized in neighboring sites (u_4, u_5) are locked into perpetual oscillations. The time evolution of the modal occupancies $|c_4|^2$ and $|c_5|^2$ is illustrated for three different ensembles as well as for the ensemble average.

thermalization and the sustainability of equilibrium below the limiting case of infinite ensembles. To explore this aspect, we analyze the evolution dynamics of the 1D Aubry-André lattice comprising 30 sites with a disorder strength $\Lambda = 5$. In the results of Fig. 1 each ensemble was initiated out of equilibrium by exciting only a subset of modes, differentiated only by the modal phases. In contrast to these results, here, we examine the statistics of an AA system by initiating each ensemble at a state with both a random phase and amplitude for each mode by respecting the two invariants, at $U = 2.3$ and $P = 2$. By utilizing a very large number of such ensembles ($N_a = 10^4$), we can verify that the ensemble average at time $t = 0$ (before initiating the simulation) corresponds exactly to the theoretically predicted RJ distribution of Eq. (2). In this regard, we can employ such a combination of random initial states to successfully initiate a system extremely close to the theoretically predicted RJ equilibrium.

Figures 2(a) and 2(b) illustrate the thermal evolution for a low disorder ($\Lambda = 1$) and a high disorder ($\Lambda = 5$) AA case, respectively, when initiated close to the theoretical thermal equilibrium at $T = -0.44$. In the first scenario, the system remains at equilibrium for all subsequent observation times, in accord with the theoretical assertions of optical thermodynamics (i.e., the value of the optical entropy can never decrease). On the other hand, the results for the strongly disordered lattice diverge noticeably. The system gradually deviates from its theoretically predicted equilibrium by forming localized ridges in the averaged spectra and remains indefinitely in a newly formed state. This particular result can be replicated exactly by increasing the ensemble number to $N_a = 10^5$, indicating that this effect might persist even close to the limit of infinite ensembles. This is a possible indication that localization might prevent the system from exploring its entire phase space in a fully fair and ergodic manner in finite timescales. While this breakdown is not severe, it remains relevant to the problem discussed herein. Similar effects can be observed for other 1D and 2D cases.

To delve deeper into the origin of these effects we focus on two out of the 30 eigenmodes of the system, in particular u_4 and u_5. These two eigenmodes correspond to neighboring localized states, as shown in Fig. 2(c). Considering the strong local overlap of their intensity profiles as well as the small separation in energy, their mutual nonlinear coupling is expected to dominate the local dynamics. The lower panel of Fig. 2(c) illustrates the evolution of the modal occupancies $|c_4|^2$ and $c_5|^2$, as an average over all N_a ensembles. Evidently, the two modal amplitudes transition from their initial thermal values to a nonthermal equilibrium state. In addition, the power variations in each mode mirror the fluctuations in the other, revealing their strong mutual coupling. A similar response is

also observed in the temporal evolution of individual ensembles, as illustrated in the same figure. However, in contrast to the ensemble average, each individual ensemble sustains a continuous oscillation between the two modes. This behavior is observed consistently in all ensembles, which indicates that the system might remain practically indefinitely in this dynamic phase, considering the already very high value of N_a. It therefore becomes apparent that emergent oscillations between neighboring localized states can distinctly alter the nonequilibrium response of strongly disordered classical lattices. In general, such clusters of strongly coupled modes can involve three or even more localized states.

III. PRETHERMALIZATION PHENOMENA UNDER STRONG DISORDER

Of interest would be to explore the thermal response of disordered lattices when U is not conserved. Under slowly varying conditions, the optical temperature T can be calculated from the instantaneous value of U, at each time t, thereby predicting the form of a possible prethermal RJ distribution. We consider an example where energy is exchanged with a heat bath, and a time-periodic lattice where energy is absorbed by the drive.

In our heat bath example, we consider two different species for the optical field which here correspond to two different circular polarizations of light (left- and right-handed). Nonlinear interaction between the two species are enabled via cross phase modulation effects. Here, the two polarizations $a^R_{i,j}$ and $a^L_{i,j}$ obey separately Eq. (1), and also involve an additional term of the form $\gamma|a^{R(L)}_{i,j}|^2 a^{L(R)}_{i,j}$. This term allows for an exchange between the internal energies U_L and U_R of these two species, leading to a system of two nonlinearly coupled equations,

$$i\partial_t \alpha^L_{i,j} = \beta_{ij}\alpha^L_{i,j} + \sum_{k,l}\kappa_{ij,kl}\alpha^L_{k,l} + \left|\alpha^L_{i,j}\right|^2\alpha^L_{i,j} + \gamma\left|\alpha^R_{i,j}\right|^2\alpha^L_{i,j} = 0 \tag{5}$$

$$i\partial_t \alpha^R_{i,j} = \beta_{ij}\alpha^R_{i,j} + \sum_{k,l}\kappa_{ij,kl}\alpha^R_{k,l} + \left|\alpha^R_{i,j}\right|^2\alpha^R_{i,j} + \gamma\left|\alpha^L_{i,j}\right|^2\alpha^R_{i,j} = 0, \tag{6}$$

where the L and R indices specify the nature of the two species A and B. The last two terms in Eqs. (5) and (6) describe the self- and cross-phase modulation effects responsible for thermalization and energy exchange between polarizations, respectively. Here, the coefficient γ denotes the strength of the cross-phase interaction, which is typically equal to 2 for circular polarized light.

In this context, we study a 2D array with $\kappa_{i,j} = 1$ comprising 40×40 elements corresponding to a waveguide lattice able to guide both a left- and right-handed polarized light. The 39 leftmost columns comprise an ordered lattice of waveguides that support only a right-handed polarization, while the rightmost column comprises disordered waveguides that allow both polarizations [Fig. 3(a)]. In this respect, the subsystem of 40×40 sites where right-handed polarized light is supported is considered to be the optical bath, while thermalization is studied on the rightmost 1×40 disordered subsystem, associated only with the left-handed polarization.

According to classical thermodynamics, a body in contact with a heat bath will exchange energy and will eventually attain the temperature of the bath T_{HB}. This process is first investigated for the 1D Anderson lattice for $\Lambda = 1$. The heat bath is initiated directly at equilibrium, at $T_{HB} = -0.17$, while the small subsystem is initiated at an out-of-equilibrium state with an expected $T_s = -0.87$ (calculated from U_s and P_s at $t = 0$). Figure 3(b) illustrates the thermal evolution of the disordered subsystem and the gradual relaxation of its temperature to T_{HB}.

Next, we investigate the same problem for a much stronger disorder ($\Lambda = 8$). We excite four eigenstates of the 1D lattice that correspond to eigenmodes tightly confined in neighboring sites and therefore are highly coupled. During evolution, the heatmbath quickly thermalizes the four excited eigenmodes, resulting in a prethermal RJ distribution that applies exclusively to these modes, while no power is exchanged with the rest of the 1D lattice. The temperature T of this state is explicitly calculated from the instantaneous U of the subsystem comprising the four modes, while the brown curves are obtained analytically. The fact that the RJ curves perfectly match the quasi-equilibria of the blue surface plot suggest the onset of prethermalization. The right panel of Fig. 3(c) shows the temperature of the full disordered system T_S as well as the temperature of the subsystem T_{SS}, which evolves into T_{HB}. In general, we assume that the state observed in Fig. 3(c) will remain active until power eventually spreads to the remaining 26 modes, an exponentially slower process. In this respect, it becomes apparent that for a high enough cross-species interaction strength γ, a heat bath can rapidly prethermalize local subsystems of a disordered lattice, effectively circumventing the thermal slowdown experienced by the rest of the system.

Another class of configurations that does not maintain energy invariance and can exhibit prethermalization is that of time-driven (Floquet) systems [40–45]. Floquet lattices manifest self-heating, wherein they gradually drive themselves into an infinite temperature state through their own nonlinear dynamics. In other words, time-driven systems tend to perpetually absorb energy from their own lattice variations, thus changing their internal energy. To investigate this class of effects, we study a diatomic topological lattice with a periodic square unit cell. The two main sites per unit cell are shown in blue and red in Fig. 3(d). The lattice comprises 61 sites and follows the dynamics of Eq. (1). In contrast to our previous examples where κ were uniform and normalized to unity, now we define four alternating coupling terms that vary sinusoidally, i.e., $\kappa_n = \sin(2\pi t/T_f + \phi_n)$ with $\phi_n = \phi_{n+1} + \pi/2$ a rotating phase shift. This leads to a quasi-spectrum with two topological edge states at the Floquet gap above a certain T_f, a scheme demonstrated in various photonic realizations [46,47].

In Fig. 3(e) we demonstrate the self-heating process for $\Lambda = 0$, where U is no longer conserved but gradually drops to zero towards an infinite temperature state, associated with modal equipartition. The system is initiated at a prethermalized RJ state, with T and μ calculated from the instantaneous

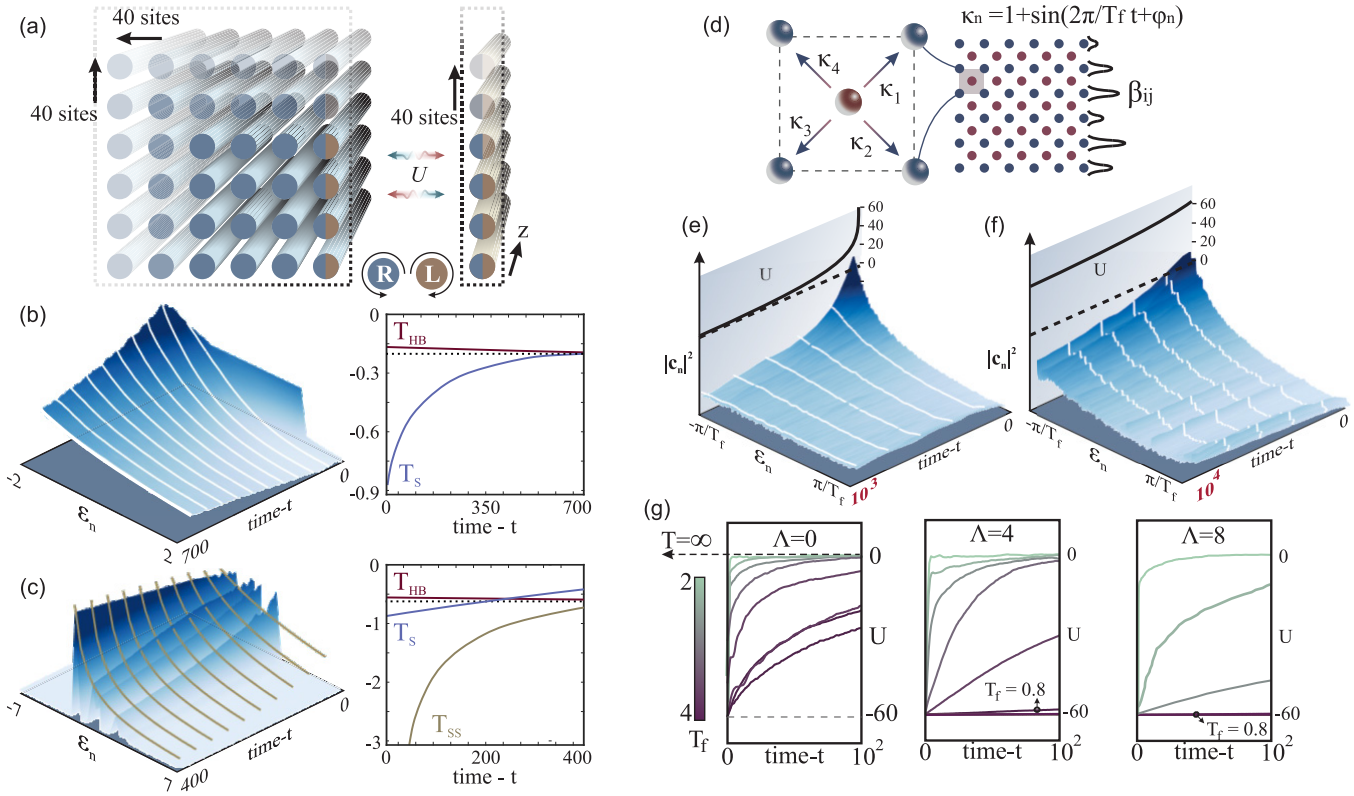

FIG. 3. (a) A 40×40 waveguide lattice is divided into a 1×40 disordered sublattice that supports both left- and right-handed polarized light. The remaining 39×40 supports only right-handed polarized waves. Information as to thermalization of the subsystem is obtained only from the left-handed polarization of the sublattice, while the remaining system represents a heat bath. (b) Thermal evolution (left) and relaxation of temperature (right) for $\Lambda = 1$. The disordered sublattice's temperature T_S relaxes into the temperature of the bath T_{HB}. (c) Thermal evolution (left) and relaxation of temperature (right) for $\Lambda = 8$. The heat bath will prethermalize the subsystem involving only these four modes. (d)–(f) A disordered Floquet square lattice. The couplings are modulated sinusoidally in time. (d) The Floquet lattice with no disorder self-heats into an infinite temperature after initiated at a prethermal RJ distribution. (e) A Floquet lattice with Anderson disorder self-heats at a greatly reduced pace. (f) Self-heating in a Floquet array for various T_f and Λ.

energy U, associated with the Floquet quasi-spectrum of the disordered Hamiltonian $H_{\text{eff}} = i/T_f \log[U_M(T)]$, with $U_M = -i\int_o^t dt' H(t')$ the unitary operator and H the instantaneous linear Hamiltonian of Eq. (1). Next, we study localization effects by including Anderson disorder. Linear diagonalization reveals that the degree of eigenmode localization is correlated not only to the strength of the disorder Λ but also to the period of modulation T_f. This indicates that T_f might antagonize Λ in slowing down thermalization. Figure 3(f) demonstrates the relaxation dynamics of the lattice at $\Lambda = 4$. Evidently, the self-heating process slows down and U remains closer to its initial value for a much longer time, while a prethermal RJ state manifests at all times.

To quantify the relaxation times of U, we must account for both Λ and T_f. In Fig. 3(g) we plot the variation of the internal energy for a delocalized ($\Lambda = 0$), moderately localized ($\Lambda = 4$), and strongly localized case ($\Lambda = 8$) for different T_f. For a small enough period ($T_f = 2$), in all cases, the Floquet lattices reach an infinite temperature at a relatively fast rate, while, in contrast, high T_f values can stabilize the system almost indefinitely in the presence of strong disorder. It becomes clear, therefore, that photonic systems that manifest both localization and time periodicity can avoid self-heating, while manifesting stable prethermal Rayleigh-Jeans states for very long times, with T and μ associated with the instantaneous U.

ACKNOWLEDGMENTS

This work was partially supported by ONR MURI (Grant No. N00014-20-1-2789), AFOSR MURI (Grants No. FA9550-20-1-0322 and No. FA9550-21-1-0202), the National Science Foundation (Grants No. DMR-1420620 and No. EECS-1711230), the MPS Simons Collaboration (Simons Grants No. 733682 and No. 733698), the W. M. Keck Foundation, the US-Israel Binational Science Foundation (Grant No. 2016381), and the US Air Force Research Laboratory (Grant No. FA86511820019). G.G.P acknowledges the support of the Bodossaki Foundation.

APPENDIX A: THE RAYLEIGH-JEANS DISTRIBUTION

We consider a microcanonical ensemble of a conservative optical system with a finite number of modes M with energy levels ε_i, each associated with a degeneracy g_i. Let us now assume that the system is composed of $N = \sum_i n_i$ indistinguishable photons n_i at a specific wavelength distributed over g_i states with the same energy ε_i. The total energy ("optical

internal energy") is $E = -\sum_i \varepsilon_i n_i$. In such a system, the number of ways (W) in which one can arrange n_i particles within g_i levels is given by

$$W = \prod_i (n_i + g_i - 1)!/[n_i!(g_i - 1)!]. \tag{A1}$$

Maximizing the total optical entropy $S_N = \ln W$, under the two individual constrains (N and E are constants of motion), leads to a Bose-Einstein distribution

$$n_i/g_i = 1/(e^{-\alpha-\beta\varepsilon_i} - 1) \tag{A2}$$

with the help of the Stirling approximation ($\ln n! = n \ln n - n$) and by involving the Lagrange multipliers α, β. Under the condition $-\alpha - \beta\varepsilon_i \ll 1$ the Bose-Einstein distribution reduces to a Rayleigh-Jeans distribution:

$$n_i/g_i = -1/(\alpha + \beta\varepsilon_i). \tag{A3}$$

This limit is valid in the context of classical optics, considering that the number of photons (associated with the total power) is much larger than the number of available modes ($n_i/g_i \ll 1$ hence $e^{-\alpha-\beta\varepsilon_i} \to 1$). We can then promptly impose the relation $n_i/g_i = n_c|c_i|^2$, where n_c represents a proportionality factor. To reach the final form of the RJ distribution we adopt the more conventional definitions for optical temperature T and chemical potential μ, as $\alpha = \mu/(Tn_c)$, $\beta = 1/(Tn_c)$, obtaining

$$|c_i|^2 = -T/(\mu + \varepsilon_i). \tag{A4}$$

APPENDIX B: DERIVATION OF THE EQUATION OF STATE

In a finite optical system that supports M modes we employ the following definitions: the optical entropy $S = \sum_i^M \ln|c_i|^2$, the total power $P = \sum_i^M |c_i|^2$, and the optical energy $U = -\sum_i^M \varepsilon_i|c_i|^2$. Taking these expressions into account, we obtain the following expression for a system into thermal equilibrium:

$$\begin{aligned} 1/TU - P\mu/T &= 1/T \sum_i^M \varepsilon_i|c_i|^2 - \mu/T \sum_i^M |c_i|^2 \\ &= \sum_i^M \left[\varepsilon_i/(\varepsilon_i + \mu) + \mu/(\varepsilon_i + \mu)\right] = M, \end{aligned} \tag{A5}$$

which directly leads to the equation of state in its final form:

$$U - \mu P = MT. \tag{A6}$$

APPENDIX C: IMPACT OF EIGENVALUE STATISTICS

Eigenvalue statistics are important in distinguishing between thermalizing and ergodic phases in quantum lattices.

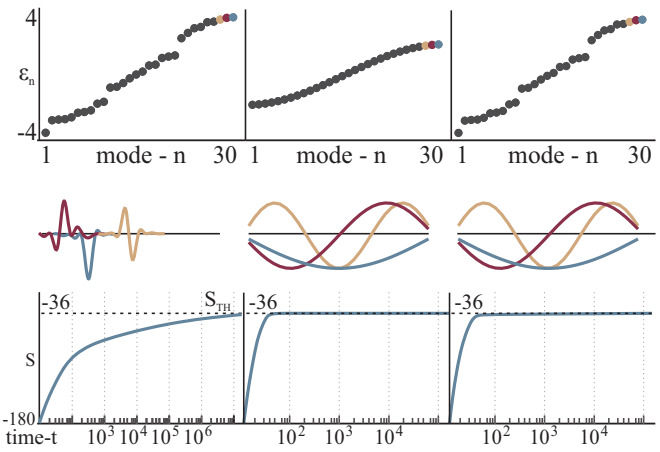

FIG. 4. Entropy maximization for an Anderson lattice with $\Lambda = 7$ (left), a 1D chain with zero disorder (middle), and a mixed lattice having exactly the same eigenvalues of the first system and the eigenmode field profiles of the second (right). Evidently, the eigenvalue statistics play a minimal role in suppressing the process of thermalization.

To highlight the fundamental difference between thermalizing quantum and optical (classical) lattices, we investigate the impact of the eigenvalue statistics in optical disordered systems by considering a similarity transformation on an Anderson optical lattice with disorder strength $\Lambda = 5$ (with $M = 30$ sites). A Hamiltonian produced under a similarity transformation retains an identical spectrum with the original Hamiltonian, albeit with different eigenmode profiles. In this respect, we consider a mixed Hamiltonian $H' = V^{-1}EV$ where E is a diagonal matrix with the eigenvalues of the disordered Anderson Hamiltonian H and V is a matrix with columns that correspond to the eigenvectors of a 1D tight-binding chain with unit couplings and zero disorder (with Hamiltonian H_0, effectively an Anderson lattice with $\Lambda = 0$). In Fig. 4 we simulate the Kerr nonlinear evolution for these three cases (disordered H, nondisordered H_0, mixed H'). First, we verify that the lattice thermalizes rapidly into a RJ distribution for the nondisordered case while thermalization times are severely suppressed for the disordered lattice. Interestingly, thermal equilibrium in the mixed (third) lattice is attained at a rate that is much closer to the nondisordered case (albeit around three times slower). It is therefore apparent that the eigenvalue statistics and therefore the phase matching conditions in the disordered spectra play a minimal role in suppressing thermalization, considering that the difference in relaxation times between the first and the third case is on the order of 10^5. Therefore, we may conclude that the origin of the thermal suppression can be attributed almost exclusively to the spatial localization of the eigenmodes.

[1] P. W. Anderson, Absence of diffusion in certain random lattices, Phys. Rev. **109**, 1492 (1958).

[2] A. Lagendijk, B. V. Tiggelen, and D. S. Wiersma, Fifty years of Anderson localization, Phys. Today **62**(8), 24 (2009).

[3] C. W. J. Beenakker, Random-matrix theory of quantum transport, Rev. Mod. Phys. **69**, 731 (1997).

[4] J. Billy, V. Josse, Z. Zuo, A. Bernard, B. Hambrecht, P. Lugan, D. Clément, L. Sanchez-Palencia, P. Bouyer, and A. Aspect, Direct observation of Anderson localization of matter waves in a controlled disorder, Nature (London) **453**, 891 (2008).

[5] G. Roati, C. D. Errico, L. Fallani, M. Fattori, C. Fort, M. Zaccanti, G. Modugno, M. Modugno, and M. Inguscio, Anderson localization of a non-interacting Bose-Einstein condensate, Nature (London) **453**, 895 (2008).

[6] H. De Raedt, A. Lagendijk, and P. de Vries, Transverse localization of light, Phys. Rev. Lett. **62**, 47 (1989).

[7] D. S. Wiersma, P. Bartolini, A. Lagendijk, and R. Righini, Localization of light in a disordered medium, Nature (London) **390**, 671 (1997).

[8] A. Lagendijk and B. A. van Tiggelen, Resonant multiple scattering of light, Phys. Rep. **270**, 143 (1996).

[9] S. M. Popoff, G. Lerosey, R. Carminati, M. Fink, A. C. Boccara, and S. Gigan, Measuring the transmission matrix in optics: An approach to the study and control of light propagation in disordered media, Phys. Rev. Lett. **104**, 100601 (2010).

[10] H. Cao, Y. G. Zhao, S. T. Ho, E. W. Seelig, Q. H. Wang, and R. P. H. Chang, Random laser action in semiconductor powder, Phys. Rev. Lett. **82**, 2278 (1999).

[11] C. Vanneste and P. Sebbah, Selective excitation of localized modes in active random media, Phys. Rev. Lett. **87**, 183903 (2001).

[12] M. Segev, Y. Silberberg, and D. N. Christodoulides, Anderson localization of light, Nat. Photon. **7**, 197 (2013).

[13] T. Schwartz, G. Bartal, S. Fishman, and M. Segev, Transport and Anderson localization in disordered two-dimensional photonic lattices, Nature (London) **446**, 52 (2007).

[14] Y. Lahini, A. Avidan, F. Pozzi, M. Sorel, R. Morandotti, D. N. Christodoulides, and Y. Silberberg, Anderson localization and nonlinearity in one-dimensional disordered photonic lattices, Phys. Rev. Lett. **100**, 013906 (2008).

[15] E. E. Morales-Delgado, S. Farahi, I. N. Papadopoulos, D. Psaltis, and C. Moser, Delivery of focused short pulses through a multimode fiber, Opt. Express **23**, 9109 (2015).

[16] I. N. Papadopoulos, S. Farahi, C. Moser, and D. Psaltis, Focusing and scanning light through a multimode optical fiber using digital phase conjugation, Opt. Express **20**, 10583 (2012).

[17] E. Michaely and S. Fishman, Effective noise theory for the nonlinear Schrödinger equation with disorder, Phys. Rev. E **85**, 046218 (2012).

[18] S. Flach, D. O. Krimer, and C. Skokos, Universal spreading of wave packets in disordered nonlinear systems, Phys. Rev. Lett. **102**, 024101 (2009).

[19] G. Kopidakis, S. Komineas, S. Flach, and S. Aubry, Absence of wave packet diffusion in disordered nonlinear systems, Phys. Rev. Lett. **100**, 084103 (2008).

[20] V. Oganesyan, A. Pal, and D. A. Huse, Energy transport in disordered classical spin chains, Phys. Rev. B **80**, 115104 (2009).

[21] L. Amico and V. Penna, Dynamical mean field theory of the Bose-Hubbard model, Phys. Rev. Lett. **80**, 2189 (1998).

[22] A. Polkovnikov, S. Sachdev, and S. M. Girvin, Nonequilibrium Gross-Pitaevskii dynamics of boson lattice models, Phys. Rev. A **66**, 053607 (2002).

[23] G. M. Kavoulakis, Effectively attractive Bose-Einstein condensates in a rotating toroidal trap, Phys. Rev. A **69**, 023613 (2004).

[24] T. Scoquart, P.-É. Larré, D. Delande, and N. Cherroret, Weakly interacting disordered Bose gases out of equilibrium: From multiple scattering to superfluidity, Europhys. Lett. **132**, 66001 (2020).

[25] D. M. Basko, Weak chaos in the disordered nonlinear Schrödinger chain: Destruction of Anderson localization by Arnold diffusion, Ann. Phys. **326**, 1577 (2011).

[26] M. Mulansky and A. Pikovsky, Scaling properties of energy spreading in nonlinear Hamiltonian two-dimensional lattices, Phys. Rev. E **86**, 056214 (2012).

[27] N. Berti, K. Baudin, A. Fusaro, G. Millot, A. Picozzi, and J. Garnier, Interplay of thermalization and strong disorder: Wave turbulence theory, numerical simulations, and experiments in multimode optical fibers, Phys. Rev. Lett. **129**, 063901 (2022).

[28] M. Abuzarli, N. Cherroret, T. Bienaimé, and Q. Glorieux, Nonequilibrium prethermal states in a two-dimensional photon fluid, Phys. Rev. Lett. **129**, 100602 (2022).

[29] F. O. Wu, A. U. Hassan, and D. N. Christodoulides, Thermodynamic theory of highly multimoded nonlinear optical systems, Nat. Photon. **13**, 776 (2019).

[30] H. Pourbeyram, P. Sidorenko, F. O. Wu, N. Bender, L. Wright, D. N. Christodoulides, and F. Wise, Direct observations of thermalization to a Rayleigh–Jeans distribution in multimode optical fibres, Nat. Phys. **18**, 685 (2022).

[31] A. L. Marques Muniz, F. O. Wu, P. S. Jung, M. Khajavikhan, D. N. Christodoulides, and U. Peschel, Observation of photon-photon thermodynamic processes under negative optical temperature conditions, Science **379**, 1019 (2023).

[32] K. G. Makris, F. O. Wu, P. S. Jung, and D. N. Christodoulides, Statistical mechanics of weakly nonlinear optical multimode gases, Opt. Lett. **45**, 1651 (2020).

[33] A. Ramos, L. Fernández-Alcázar, T. Kottos, and B. Shapiro, Optical phase transitions in photonic networks: A spin-system formulation, Phys. Rev. X **10**, 031024 (2020).

[34] G. G. Pyrialakos, H. Ren, P. S. Jung, M. Khajavikhan, and D. N. Christodoulides, Thermalization dynamics of nonlinear non-Hermitian optical lattices, Phys. Rev. Lett. **128**, 213901 (2022).

[35] H. Ren, G. G. Pyrialakos, F. O. Wu, P. S. Jung, N. K. Efremidis, M. Khajavikhan, and D. N. Christodoulides, Nature of optical thermodynamic pressure exerted in highly multimoded nonlinear systems, Phys. Rev. Lett. **131**, 193802 (2023).

[36] M. A. Selim, F. O. Wu, H. Ren, M. Khajavikhan, and D. Christodoulides, Thermodynamic description of the near- and far-field intensity patterns emerging from multimode nonlinear waveguide arrays, Phys. Rev. A **105**, 013514 (2022).

[37] S. Aubry and G. André, Analyticity breaking and Anderson localization in incommensurate lattices, Ann. Israel Phys. Soc. **3**, 18 (1980).

[38] V. E. Zakharov, V. S. L'vov, and G. Falkovich, *Kolmogorov Spectra of Turbulence I* (Springer, Berlin, Heidelberg, 1992).

[39] A. Picozzi, J. Garnier, T. Hansson, P. Suret, S. Randoux, G. Millot, and D. N. Christodoulides, Optical wave turbulence: Towards a unified nonequilibrium thermodynamic formulation of statistical nonlinear optics, Phys. Rep. **542**, 1 (2014).

[40] A. Lazarides, A. Das, and R. Moessner, Equilibrium states of generic quantum systems subject to periodic driving, Phys. Rev. E **90**, 012110 (2014).

[41] P. Peng, C. Yin, X. Huang, C. Ramanathan, and P. Cappellaro, Floquet prethermalization in dipolar spin chains, Nat. Phys. **17**, 444 (2021).

[42] B. Gadway, J. Reeves, L. Krinner, and D. Schneble, Evidence for a quantum-to-classical transition in a pair of coupled quantum rotors, Phys. Rev. Lett. **110**, 190401 (2013).

[43] A. Haldar, R. Moessner, and A. Das, Onset of Floquet thermalization, Phys. Rev. B **97**, 245122 (2018).

[44] R. Gawatz, A. C. Balram, E. Berg, N. H. Lindner, and M. S. Rudner, Prethermalization and entanglement dynamics in interacting topological pumps, Phys. Rev. B **105**, 195118 (2022).

[45] D. A. Abanin, W. De Roeck, W. W. Ho, and F. Huveneers, Effective Hamiltonians, prethermalization, and slow energy absorption in periodically driven many-body systems, Phys. Rev. B **95**, 014112 (2017).

[46] L. J. Maczewsky, J. M. Zeuner, S. Nolte, and A. Szameit, Observation of photonic anomalous Floquet topological insulators, Nat. Commun. **8**, 13756 (2017).

[47] G. G. Pyrialakos, J. Beck, M. Heinrich, L. J. Maczewsky, N. V. Kantartzis, M. Khajavikhan, A. Szameit, and D. N. Christodoulides, Bimorphic Floquet topological insulators, Nat. Mater. **21**, 634 (2022).